Effect of tissue parameters on skin heating due to millimeter EM waves

Published paper @DOI: 10.1109/TMAG.2014.2363898.

Effect of tissue parameters on skin heating due to millimeter EM waves

Luca Zilberti[1], Damien Voyer[3], Oriano Bottauscio[1], Mario Chiampi[2], Riccardo Scorretti[3]

[1]Istituto Nazionale di Ricerca Metrologica, Strada delle Cacce 91, 10135 Torino, Italy
[2]Politecnico di Torino, C.so Duca degli Abruzzi 24, 10129 Torino, Italy
[3]Université de Lyon – Ampère (CNRS UMR5005, École Centrale de Lyon, INSA-Lyon, UCBL), F-69134 Écully Cedex, France
l.zilberti@inrim.it

***Abstract*— This paper investigates the influence of electrical and thermal human tissue parameters on the heating of a body illuminated by a millimeter plane electromagnetic wave. A stochastic approach is considered with a three-layer model of the body: it is found that the parameters of skin play a major role.**

***Index Terms*—dosimetry, millimeter wave propagation.**

I. Introduction

Nowadays millimeter and submillimeter electromagnetic (EM) waves are more and more employed in industrial environments [1], security devices (e.g. body-scanners) [2] and biomedical procedures [3-5]. For this reason, the investigation of their biological effects and consequences on human health has become a hot topic, faced from different viewpoints [6-7]. Since the measurement of the dosimetric quantities induced inside a human body is practically unfeasible, computational models can be adopted to estimate the power density deposited by the EM wave into the tissues, as well as the corresponding temperature elevation. As an alternative, suitable tissue phantoms can be used to bypass the problem and carry out experimental measurements; also in this case specific mathematical models appear to be fundamental in phantom design, anyway. When mimicking the exposure of real biological tissues, a critical point shared by all computational and experimental approaches is given by the choice of the dielectric and thermal properties to be assigned to the tissues themselves. As discussed in a previous work [8], quite large uncertainties and spread of such values are found among scientific articles, due to natural variability, sample features and measurement conditions. Therefore, parametric analyses are strongly useful to investigate the influence of tissue parameters in the thermal response of the body. On the other hand, an accurate investigation of field propagation is a computationally demanding task in the frequency band of interest [9], insomuch that numerical solver fails have been reported in some cases [10].

II. Method

On the basis of the formulations proposed in [8], the present work uses a 1D model to evaluate the heating of tissues, represented as a stratified structure with 3 flat layers indefinite over the *xy* plane: skin, subcutaneous adipose tissue (SAT) and muscle. This structure is exposed for a limited time to a linearly polarized uniform plane wave, with a frequency of 0.1 THz or 1 THz, carrying a unitary power density and

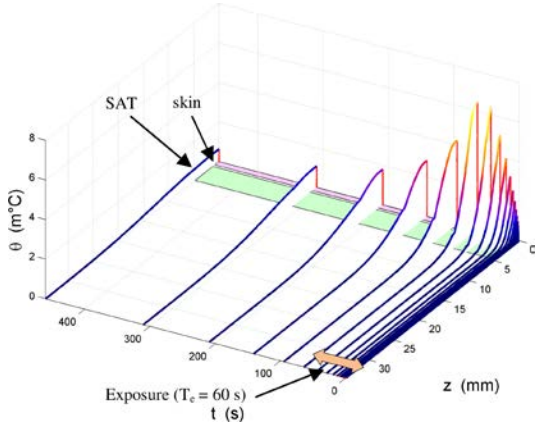

Fig 1: Spatial distribution of θ (m°C) as a function of time for the reference case (frequency = 1 THz, exposure time = 60 s).

normally incident to the body surface (i.e. travelling along the *z*-axis). Under these conditions, disregarding any initial transient and working in frequency domain, the propagation of the electric (*E*) and magnetic (*H*) fields in each *i*-th layer (including the external air region) is described by 1D Helmholtz equations. These latter can be solved analytically, by exploiting the electric field of the unperturbed wave as a driving term, considering that no reflection takes place in the last layer (which extends to infinite) and imposing classical continuity conditions (i.e. conservation of both *E* and *H* tangential components) across each interface [8]. Thus, the average volume power density P_{em} transferred by the field to the tissues at each period is given by:

$$P_{em}(z) = \frac{\sigma(z)\left|E(z)\right|^2}{2} \tag{1}$$

where σ indicates the electric conductivity. Then, P_{em} becomes the source term for the bioheat equation [11], which is formulated in terms of temperature elevation θ with respect to the starting steady-state temperature (that varies along *z*), avoiding any assumption on the values of metabolic power and blood temperature:

$$\frac{\partial}{\partial z}\left(\lambda\frac{\partial\theta}{\partial z}\right) - h_b\theta + P_{em} = c_v\frac{\partial\theta}{\partial t} \tag{2}$$

where λ is the thermal conductivity, h_b is the perfusion coefficient, c_v is the heat capacity per unit volume and *t* is time. Equation (2), subjected to Robin boundary conditions at the border with air (with heat transfer coefficient set to

7 Wm^{-2} $°C^{-1}$) and continuity conditions across the interfaces, is finally solved by a homemade code based on the Finite Element Method in the time domain, through a time-stepping Crank–Nicolson procedure.

A phase of active exposure followed by a "cooling period" of 400 s is simulated and the maximum temperature elevation θ_{max} is analyzed (see Fig. 1). Unlike the deterministic approach followed in [8], a stochastic method based on a polynomial chaos expansion of θ_{max} (see appendix) is here exploited to reduce the computational burden. The computations have been performed by using a 3rd and 4th order developments: the results are stable, compared with those obtained with a development of higher order (not shown for brevity). The computational times are reduced of many orders of magnitude with respect to a classical Monte Carlo approach: in most cases, 250 deterministic simulations (about 10 minutes on a standard PC) have been found enough to solve the stochastic problem with a 3rd order development, and no more than 2000 with a 4th order development. Most importantly, the analysis of the variance provides useful information that can be exploited to better understand the phenomenon.

III. Results of Variability

The input parameters (including the relative permittivity ε_r) reported in Table I are taken into account by using a stochastic spectral method [12, 13]; their values are varied according to the variability found in literature [8], assuming that all these parameters are independent and follow a uniform distribution. The ranges of variation of thermal parameters have been deduced from the extreme values found in literature; it must be noted that the reference values (indicated between brackets in Table I) do not necessarily correspond to the mean values of the considered ranges, but they have been chosen because they appear to be the most commonly used. As regards the permittivity and conductivity of the skin, a range of ±50% has been arbitrarily chosen. Since the penetration depth of the electromagnetic waves is very shallow at the considered frequencies, the dielectric parameters of SAT and muscle play a minor role; therefore they have been excluded from the analysis. The influence on the maximum temperature elevation θ_{max} in the skin and in the SAT is investigated for an exposure time T_e of 1 s, 10 s and 60 s. For each studied variable, the probability distribution function (PDF), as well as the partial variance and the total effect (cf. appendix) are computed. All the quantities are expressed in terms of a relative variation ($\Delta\theta_{max}$) with respect to the nominal case obtained with the reference values of the parameters.

TABLE I
Range of Variation for the Parameters. In Brackets the Reference Values.

		Skin	SAT	Muscle
ε_r	0.1 THz	2.8 – 8.4 (5.6)	3.67	8.63
	1 THz	1.43 – 4.29 (2.86)	2.50	3.20
σ (Sm^{-1})	0.1 THz	19.7 – 59.1 (39.4)	10.6	62.5
	1 THz	22.4 – 67.2 (44.8)	41.9	59.4
λ ($Wm^{-1}°C^{-1}$)		0.32 – 0.50 (0.37)	0.16 – 0.50 (0.21)	0.32 – 0.56 (0.49)
h_b ($kWm^{-3}°C^{-1}$)		3.34 – 12.3 (7.44)	1.15 – 4.75 (1.90)	1.31 – 6.49 (2.69)
c_v ($MJm^{-3}°C^{-1}$)		3.46 – 4.12 (3.76)	1.47 – 3.08 (2.14)	2.73 – 4.48 (3.73)
Thickness (mm)		1 – 4 (1)	1.5 – 10 (3.5)	∞

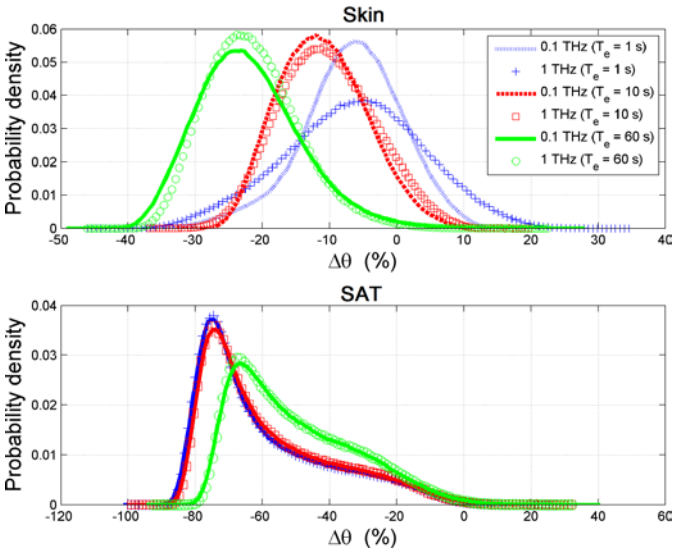

Fig 2: PDF of $\Delta\theta_{max}$ for the skin (top) and the SAT (bottom) for a frequency of 0.1 THz (continuous lines) and 1 THz (dashed lines), and for an exposure time of 1 s (blue), 10 s (red) and 60 s (green).

A. Effect of the frequency

The PDF of $\Delta\theta_{max}$ computed for the skin and the SAT at the frequencies of 0.1 THz and 1 THz are depicted in Fig. 2 for the different exposure times (1 s, 10 s and 60 s). It can be observed that the skin appears to be more sensitive to the frequency, in particular for an exposure time of 1 s. Conversely, the PDF of the SAT appears to have a little dependence on the frequency of the electromagnetic wave. It is interesting to note that in most cases $\Delta\theta_{max}$ is negative, meaning that the values assumed as reference for the parameters give rise to quite severe exposure conditions.

The analysis of the variance for skin (Table II) and SAT (Table III) puts in evidence the fact that the most important parameters are the dielectric properties of the skin, ε_r and σ (which strongly depend on the frequency), as well as the thermal conductivity. Conversely, the heating of the SAT is mostly determined by the thickness of the skin.

Together, these data support the idea that heating in the skin is dominated by the *deposition of energy* given by the electromagnetic wave, whereas in the underlying SAT *heat transfer* is the most important phenomenon.

For what concerns the skin, one observes that permittivity ε_r and conductivity σ are likely to have a joint effect: this can be deducted by the fact that for both (and only) these parameters the partial variance is significantly lower than the total effect. This sounds correct from the physical point of view: remember that the analytical expression of the solution of the Helmholtz equations in the harmonic regime [8] is given in terms of the intrinsic impedance $\underline{\eta}$ and of the propagation coefficient $\underline{k}$ of the layers:

$$\underline{\eta} = \sqrt{\frac{\mu}{\varepsilon - j\sigma/\omega}} \quad ; \quad \underline{k} = \omega\sqrt{\mu(\varepsilon - j\sigma/\omega)} \tag{3}$$

where ω is the angular frequency and the underlined symbols indicate complex quantities.

As for the SAT, even if the dielectric properties are very different at 0.1 THz and 1 THz (Table I), little or no effect is observed on the PDF. One observes that in the SAT the maximum temperature elevation is located at the interface with skin (not shown): that could explain why the thickness of the skin is determinant.

B. Effect of the exposure time

The exposure time T_e appears to have a much higher influence on the results. The analysis of variances reveals that the parameters responsible for the variability are not the same for "short" (1 s and 10 s) and "long" (60 s) exposure times.

As regards the skin, short exposure times are mainly influenced by the dielectric properties, whereas for longer exposure times the influence of thermal properties dominates: this is particularly evident at 1 THz. This suggests that for short exposure times the maximum overheating of the skin is determined by the spatial distribution of the deposited electromagnetic energy, whereas for longer times heat transfer phenomena becomes more important. As for the SAT, one observes (Figure 2) that a little difference is found between the PDFs for the exposure times of 1 s and 10 s, and the PDF for 60 s. This fact is explained by the duration of the transient for the heat conduction [18], which can be estimated as:

$$\tau = \frac{e^2}{a} \cong 40\,\text{s} \tag{4}$$

where $a = \lambda / c_v \cong 10^{-7}\ \text{m}^2\text{s}^{-1}$ is the thermal diffusivity and $e \cong 2$ mm is the thickness of the skin layer. One observes that 1 s and 10 s are much smaller than this characteristic time: therefore the heat pulse has not sufficient time to reach the SAT layer, whereas for an exposure time of 60 s this is not the case.

IV. Conclusions

The effect of the variability of some relevant parameters on the heating of the surface tissues in a human body illuminated by a plane millimeter/submillimeter wave has been taken on. The main outcome is that the variability on θ_{max} in the skin depends mostly on the electric/dielectric properties, whereas in the SAT it depends essentially on the thickness of the skin. In any case, the reference case appears to be very conservative, in that the PDFs (Figure 2) are strongly biased toward negative variations (i.e. lower temperatures). These results confirm what has been found in a previous study [8]. The exposure time appears to have a higher impact on the results than the frequency of the electromagnetic wave (of course the *absolute* value of the temperature are much higher for 1 THz than for 0.1 THz). A large difference is observed between short and long exposure times: it would be interesting to monitor the evolution of the partial variances with respect to the time, to have a better understanding of the underlying physics.

One of the major problems with this (and indeed any other) approach is the characterization of the variability of input variables. In particular, it is assumed that all the parameters are independent, which is a very conservative assumption: at the present time, this is the only possible approach, due to the lack of information on the correlation of these parameters (for instance, "high" values of some thermal parameters for one

TABLE II
PARTIAL VARIANCE (%) / TOTAL EFFECT (%) FOR THE SKIN

Parameter		0.1 THz	1 THz
ε_r skin	1s	28.2 / 36.2	33.9 / 34.8
	10 s	9.3 / 15.7	28.3 / 29.3
	60 s	2.2 / 4.6	15.3 / 15.8
σ skin	1s	20.8 / 29.1	37.5 / 38.7
	10 s	17.6 / 24.0	6.15 / 7.16
	60 s	28.3 / 30.9	0.26 / 0.67
λ skin	1s	23.3 / 23.9	18.9 / 19.5
	10 s	48.8 / 49.2	50.3 / 50.6
	60 s	18.3 / 19.1	25.5 / 26.4
c_v skin	1s	18.9 / 19.0	8.06 / 8.10
	10 s	15.2 / 15.3	11.7 / 11.7
	60 s	5.6 / 5.7	6.55 / 6.65
c_v SAT	1 s	0.0 / 0.0	0.0 / 0.0
	10 s	0.0 / 0.0	0.0 / 0.0
	60 s	1.96 / 3.47	2.14 / 4.00
Thickness skin	1s	0.30 / 0.36	0.26 / 0.36
	10 s	2.3 / 2.5	2.09 / 2.29
	60 s	27.4 / 34.2	33.7 / 41.7

TABLE III
PARTIAL VARIANCE (%) / TOTAL EFFECT (%) FOR THE SAT

Parameter		0.1 THz	1 THz
σ skin	1 s	2.11 / 2.60	0.039 / 0.049
	10 s	2.27 / 2.77	0.042 / 0.052
	60 s	3.79 / 4.32	0.07 / 0.09
λ SAT	1 s	1.85 / 2.25	1.88 / 2.28
	10 s	2.06 / 2.51	2.08 / 2.54
	60 s	4.45 / 5.41	4.57 / 5.54
Thickness skin	1 s	92.7 / 93.8	94.7 / 95.6
	10 s	92.2 / 93.4	94.4 / 95.3
	60 s	86.8 / 88.5	90.0 / 91.5
c_v skin	1 s	0.72 / 0.89	0.73 /0.89
	10 s	0.72 / 0.85	0.74 / 0.86
	60 s	0.71 / 0.75	0.73 / 0.77
c_v SAT	1 s	0.75 / 0.94	0.76 / 0.95
	10 s	0.82 / 1.04	0.83 / 1.05
	60 s	1.52 / 1.88	1.56 / 1.93

layer could statistically correspond to “high” values of another layer). These results have been obtained by using an extremely simple 1D model because of the low penetration depth in biological tissues at the frequency of interest. In future works, these results could be used to obtain a “surrogate” model of the thermal source for more realistic computations.

ACKNOWLEDGMENTS

This research is partially granted by the LABEX PRIMES (ANR-11-LABX-0063). Moreover, this work was developed under the European Metrology Research Program (EMRP)-NEW07 Joint Research Project (JRP) “Microwave and terahertz metrology for homeland security” (2012–2015). EMRP is jointly funded by the EMRP participating countries within EURAMET and the European Union.

APPENDIX: STOCHASTIC SPECTRAL METHOD

A. Polynomial chaos

The stochastic spectral method is based on the expansion of the random variable $\Delta\theta_{\max}$ in a polynomial basis depending on the 13 input random variables (Table I). Since the input random variables are characterized by uniform laws, it can be efficiently expanded on the generalized polynomial chaos [14] based on the Legendre polynomials:

$$\Delta\theta_{\max} = \sum_{\mathbf{i}\in\mathbb{N}^{13}} y_{\mathbf{i}}\psi_{\mathbf{i}}(\xi) \quad \text{with: } \psi_{\mathbf{i}}(\xi) = \prod_{k=1}^{13} L_{i_k}(\xi_k) \qquad (5)$$

where $L_p(.)$ are Legendre polynomials, and $\xi_k \sim \mathcal{U}(-1;1)$ is a random variable, uniformly distributed between -1 and 1. The unknown coefficients y_i can be computed by using a projection method:

$$y_i = \frac{\mathrm{E}[\Delta\theta_{\max}\psi_{\mathbf{i}}]}{\mathrm{E}[{\psi_{\mathbf{i}}}^2]} = \frac{1}{\mathrm{E}[{\psi_{\mathbf{i}}}^2]}\int_{[-1;1]^{13}} \Delta\theta_{\max}(\xi)\psi_{\mathbf{i}}(\xi)\frac{1}{2^{13}}d\xi \qquad (6)$$

where E[.] is the operator expectation. The term $\mathrm{E}[{\psi_{\mathbf{i}}}^2]$ does not depend on random variables, and therefore it is computed analytically, but for the second integral quadrature rules are applied. However, applying a tensor product design based on one-dimensional Gaussian quadrature rules is most of the time prohibitive since the number of quadrature nodes increases exponentially with the number of dimensions. This number can be dramatically reduced using a sparse grid: that is, the high-order terms are dropped in (5), thus reducing the number of unknown coefficients y_i to be computed. In particular, all the terms for which the partial degree $d_i = \sum_{k=1}^{13} i_k$ is higher than a given value are dropped. A further reduction of the computational cost is obtained by using adaptive strategies [13], which consist in truncating the expansion (5) along a variable if no appreciable increase of the variance is observed.

B. Partial variance, total effect

Let $V = \mathrm{var}[\Delta\theta_{\max}]$ be the (total) variance of an observed variable $\Delta\theta_{\max}$. The variance can be written as [15, 16]:

$$V = V_0 + \sum_{i=1}^{n} V_i + \sum_{i=1}^{n}\sum_{j=i+1}^{n} V_{ij} + \ldots + V_{12\ldots n} \qquad (7)$$

where: $\mathrm{E}[V_{i\ldots}] = 0$ for any combination of indexes excepted V_0. For each variable input parameter x_i, the method computes the *partial variance* (called also *main effect* or *Sobol sensitivity index* [17]):

$$S_i = \frac{\mathrm{var}[\mathrm{E}[\Delta\theta_{\max} \mid x_i]]}{V} = \frac{V_i}{V} \qquad (8)$$

The partial variance quantifies the influence of a parameter x_i “by its own” – that is without considering the possible interactions with other parameters. The *total effect* T_i quantifies the influence of a parameter, including its possible interactions with other variables [15]:

$$T_i = 1 - \frac{\mathrm{var}[\mathrm{E}[\Delta\theta_{\max} \mid \sim x_i]]}{V} \geq S_i \qquad (9)$$

where $\mathrm{var}[\mathrm{E}[\Delta\theta_{\max} \mid \sim x_i]]$ is the variance of the conditional expectation of $\Delta\theta_{\max}$, where all parameters but x_i are known. If $T_i \simeq S_i$, the effect of x_i on $\Delta\theta_{\max}$ is nearly uncorrelated of all the other parameters.

REFERENCES

[1] C. Jansen, S. Wietzke, O. Peters, M. Scheller, N. Vieweg, M. Salhi, N. Krumbholz, C. Jördens, T. Hochrein, M. Koch, “Terahertz imaging: Applications and perspectives”, *Appl Opt*, vol. 49, pp. E49-E57, 2010.

[2] R. Appleby, B. Wallace, “Standoff detection of weapons and contraband in the 100 GHz to 1 THz region”, *IEEE Trans Antennas Propag*, vol. 55, pp. 2944-2956, 2007.

[3] M. Logani, I. Szabo, V. Makar, A. Bhanushali, S. Alekseev, M. Ziskin, “Effect of millimeter wave irradiation on tumor metastasis”, *Bioelectromagnetics*, vol. 27, pp. 258-264, 2006.

[4] Y. Sun et al., “A promising diagnostic method: Terahertz pulsed imaging and spectroscopy”, *World J. Radiol*. vol. 28, n. 3, pp. 55-65, 2011.

[5] E. Pickwell, V. Wallace, “Biomedical applications of terahertz technology”, *J Phys D Appl Phys*, vol. 39, pp. 301-310, 2006.

[6] G.J. Wilmink, J. E. Grundt, “Current state of research on biological effects of terahertz radiation,” *Journal of Infrared, Millimeter and Terahertz Waves*, vol. 32, n. 10, pp. 1074-1122, 2011.

[7] E. Pickwell, B.E. Cole et al., “In vivo study of human skin using pulsed terahertz radiation,” *Phys. Med. Biol.*, vol. 49, pp. 1595-1607, 2004.

[8] L. Zilberti, A. Arduino, O. Bottauscio, M. Chiampi, “Parametric Analysis of Transient Skin Heating Induced by Terahertz Radiation,” *Bioelectromagnetics*, vol. 35, n. 5, pp. 314-323, 2014.

[9] Y. Chung, C. Cheon, J. Son; S. Hahn, “FDTD analysis of propagation characteristics of terahertz electromagnetic pulses”, *IEEE Transactions on Magnetics*, vol.36, n. 4, pp. 951-955, 2000.

[10] T. Kleine-Ostmann, C. Jastrow et al., “Field Exposure and Dosimetry in the THz Frequency Range,” *IEEE Trans. Terahertz Science and Technology*, vol. 4, n. 1, pp. 12-24, 2014.

[11] H. Pennes, Analysis of tissue and arterial blood temperatures in the resting human forearm, *J. Appl. Physiol*., vol. 1, 1948.

[12] Voyer, D., Musy, F., Nicolas, L., Perrussel, R., “Probabilistic methods applied to 2D electromagnetic numerical dosimetry,” *COMPEL: The International Journal for Computation and Mathematics in Electrical and Electronic Engineering*, vol. 27, n. 3, pp. 651-667, 2008.

[13] Voyer, D., Nicolas, L., Perrussel, R., Musy, F., “Comparison of methods for modeling uncertainties in a 2d hyperthermia problem,” *Progress In Electromagnetics Research B*, vol. 11, pp. 189-204, 2009.

[14] Xiu, D., Karniadakis, G. E., “The Wiener–Askey polynomial chaos for stochastic differential equations”, *SIAM Journal on Scientific Computing*, vol. 24, n. 2, pp. 619-644, 2002.

[15] Kiebre, R. “Contribution to the modelling of aircraft tyre-road interaction”, chap. 5 (Doctoral dissertation, Université de Haute Alsace-Mulhouse), 2010.

[16] Sudret, B., “Global sensitivity analysis using polynomial chaos expansions”, *Reliability Engineering & System Safety*, vol. 93, n.7, pp. 964-979, 2008.
[17] Sobol, I.M. “Global sensitivity indices for nonlinear mathematical models and their Monte Carlo estimates,” *Mathematics and computers in simulation*, vol. 55, n.1-3, pp. 271-280, 2001.
[18] Tsacalos D., “Diffusivité thermique”, *Techniques de l’ingénieur*, r2950, 1984.